Collision-induced rototranslational spectra of H_2-He from an accurate *ab initio* dipole moment surface

Wilfried Meyer
Fachbereich Chemie, Universität Kaiserslautern, 675 Kaiserslautern, Federal Republic of Germany

Lothar Frommhold
Physics Department, University of Texas at Austin, Austin, Texas 78712-1081
(Received 21 April 1986)

For the study of collision-induced dipole moments, the collisional H_2-He complex is treated as a molecule in the self-consistent-field and size-consistent coupled electron pair approximations. The basis set accounts for 95% of the correlation energies and separates correctly at distant range. The vibrational average ($v=v'=0$) of the induced dipole components is obtained and recast in a simple but accurate analytical representation. It is used for computations of the spectral moments and spectral profile of the collision-induced rototranslational spectra of H_2-He. The computations are in close agreement, on an absolute intensity scale, with Birnbaum's measurements at 77, 195, and 292 K of such spectra. The fundamental theory is thus seen to predict these spectra reliably even when the anisotropy of the potential is neglected, probably with an accuracy of better than 5%, over the frequency band from 0 to $\sim 2000\ cm^{-1}$.

I. INTRODUCTION

The atmospheres of the outer planets consist of hydrogen with a small helium admixture. Both gases are infrared inactive but the collisional pairs, H_2-H_2 and H_2-He, have characteristic dipole spectra which render these atmospheres opaque in the far-infrared region.[1-4] Accurate knowledge of the collision-induced rototranslational spectra of hydrogen and helium is essential for the determination of the vertical temperature profile of these atmospheres, the measurement of the helium-to-hydrogen abundance ratio, the analysis of the Voyager infrared interferometer spectrometer (IRIS) spectra, and a general understanding of the collision-induced spectra from first principles.

A previous investigation[5] developed the theory of spectral line shape of the binary collision-induced rotovibrational (CIRV) spectra of systems like H_2-He. Numerical computations of the collision-induced rototranslational absorption (CIRTA) spectra of H_2-He were based on advanced isotropic interaction potentials[6,7] and Wormer and van Dijk's self-consistent-field (SCF) dipole moments[8] for equilibrium separation of H_2. The resulting computational spectra are in rough agreement with Birnbaum's measurement,[4] but are consistently too weak by about 20%.[5] Because of the fundamental importance of the H_2-He system, it is desirable to understand the nature of these deviations. While it is possible that the uncertainty of the interaction potentials,[6,7] or of the measurements,[4] or perhaps the neglect of the anisotropy of the interaction potential, could be responsible for the observed discrepancies, we find it promising to study here two more likely causes, namely the effects of electron correlation on the induced dipole moment and vibrational averaging, which have not been considered in previous work.

We present a new computation of the induced H_2-He dipole moment based on highly correlated wave functions (Sec. II). In Sec. III, these data are used, along with an advanced isotropic potential,[7] to compute CIRTA spectra for comparison with the previous computations[5] and the measurements.[4]

II. *Ab initio* DIPOLE MOMENT FUNCTION

The determination of collision-induced dipole moments poses problems similar to the ones encountered in *ab initio* calculations of van der Waals potentials. The dipole moments are rather small and arise from very minor distortions of the charge distribution. A perturbation treatment seems natural for such small effects, but it cannot deal sufficiently well with electron exchange at shorter range. On the other hand, standard quantum chemical methods, i.e., variational SCF and configuration interaction (CI) or coupled clusters treatments, suffer from the slow convergence of the dispersion contribution with basis-set size. Furthermore, the numerical significance of the small net effects is limited by the so-called basis set superposition errors, in particular at the CI level where basis sets are usually far from being complete. The theoretical attempts to determine induced dipole moments have recently been reviewed by Meyer.[9] So far, *ab initio* calculations have been limited to the SCF approximation except for our recent work on the system He-Ar,[10] and the preliminary discussion of correlation effects for H_2-He and H_2-H_2 presented in Ref. 9.

The results concerning the He-Ar (Refs. 9 and 10) system demonstrated that dipole moment contributions from both intra-atomic and interatomic electron correlation are both substantial. These are all of opposite sign so that for this particular system, they largely cancel. The basis set superposition error has effectively been avoided by basing the CI expansion on localized SCF orbitals and restricting

the configuration space for intra-atomic correlation to appropriate atomic subspaces. The resulting He-Ar dipole moment yields CIRTA intensities in agreement with the most dependable measurements.[10]

H_2-He constitutes a sufficiently small electronic system so that basis set saturation can be carried to an extent which renders the superposition error small, and thus the differences from the local CI procedure just mentioned insignificant. This system has been the first, and so far the only, molecular collisional complex for which an *ab initio* dipole moment surface has been determined. Berns *et al.*[11] used a valence-bond approach based on orbitals from the noninteracting systems in order to analyze various induction and exchange contributions to the dipole moments. They showed that the leading induction term, the dipole induced in He by the quadrupole moment of H_2, follows closely an R^{-4} dependence even at short distances. However, exchange terms become dominant for separations smaller than the collision diameter (5.71 bohrs). The dispersion contributions were found to be small everywhere. Since these calculations were limited by the nonorthogonality of the orbitals, the work seemed to suggest that better dipole moments are obtainable from simple SCF wave functions which account for induction as well as exchange effects. Such calculations have been presented by Wormer and van Dijk[8] for various H_2 orientations and bond distances. As mentioned above, these results have been used for a computation[5] of the CIRTA intensities which turned out too low by about 20%.

Part of this discrepancy may be traced to the neglect of vibrational averaging. It is well known that the computed H_2 quadrupole moment, and with it the long-range coefficient of the quadrupole-induced dipole component, come out $\sim 5\%$ greater if the vibrational average is considered instead of a "frozen" equilibrium H_2 separation.[12,13] The effects of the electron correlation on this long-range coefficient can also be estimated. Correlation increases the He polarizability by 5% but decreases the H_2 quadrupole moment by 8%,[14] yielding a net change of the leading induction term A_{23} of only -3%. Not much information exists, however, for estimating the effects of correlation and vibration on the exchange terms of the induced dipole moment.

Although the net correlation effect on the induction terms is small, it is rather demanding to account for it in an actual calculation. One has to make sure that the wave function separates properly into a product of a correlated H_2 wave function, and a correlated as well as polarized He wave function. In a CI treatment, this requires that single and double substitutions from a multiconfigurational reference wave function must be considered, which comprises all H_2 configurations that contribute significantly to the quadrupole moment. Indeed, a standard single- and double-substitution CI indicates an A_{23} induction term which is too large by 4%. In other words, it is even inferior to the SCF result. In our CI calculations we have, therefore, used the self-consistent electron pairs (SCEP) technique, which has recently been extended to the multiconfiguration reference case for an internally contracted reference function[16,17] comprising the SCF determinant $1\sigma_g^2$ and the three leading H_2 double substitutions $1\sigma_u^2$, $1\pi_u^2$, and $2\sigma_g^2$.

The basis set of Gaussian-type orbital functions (GTO's) has been carefully designed to provide accurate values for the pertinent properties of the separated systems, i.e., multipole moments and polarizabilities. Since our earlier work on the H_2-He interaction potential[7] had shown that a two-center basis of diffuse functions for H_2 has the tendency of artificially enhancing the anisotropy of polarizability and dispersion, we have used a mixed two-center—one-center basis for H_2. Thus $7s$ and $1p$ steep GTO's are attached to each proton while diffuse $2s$, $2p$, and $2d$ sets are placed at the center of the molecule. The inner s functions have been floated off the protons in order to further optimize the SCF wave function and thereby reduce basis superposition errors. For He, a $10s$, $4p$, $2d$ GTO set is used. This basis set of 52 contracted functions accounts for about 95% of the intramolecular and intermolecular correlation energies. Table I lists the GTO exponents used, and Table II displays the dipole polarizabilities and static moments obtained for He and H_2, respectively. At the CI level, all properties are in agreement with accurate values to within 1% except for the small hexadecapole moment, q_4, which deviates somewhat more. From this agreement we expect the calculated dipole moments to be correct to within 2%. Various extensions of the basis set have indeed resulted in dipole moment variations of less than 1%.

We note that for an accurate computation of the dispersion-interaction energies, the basis set used here is inferior to the one used previously for the determination of the interaction potential.[7] Thus we do not report a new potential surface here. In fact, the potential of Ref. 7 has recently been found to reproduce a variety of measurements of scattering cross sections and bulk properties very closely.[18] When the anisotropy is probed, it outperforms

TABLE I. Exponents of the GTO basis set.

He	s: $10s$ set of Huzinaga,[a] five steepest GTO's contracted
	p: 3.0,1.0,0.3 + 0.15 for p_σ
	d: 0.4
H	s: seven largest exponents of the $10s$ set of Huzinaga[a] five steepest GTO's contracted
	p: 1.2
H_2 center	s: three smallest exponents of $10s$ set of Huzinaga[a]
	p: 0.3,0.1
	d: 0.4,0.13

[a]S. Huzinaga, J. Chem. Phys. **42**, 1293 (1964).

TABLE II. Pertinent properties of He, H_2, and He-H_2 at long range, in atomic units, for $r_{H\text{-}H}=1.449$ bohrs.

		SCF	CI	Accurate[a]
He	α	1.320	1.382	1.385
H_2	$\alpha_{\parallel}$	6.773	6.765	6.766
	$\alpha_{\perp}$	4.762	4.714	4.752
	q_2	0.525	0.480	0.484
	q_4	0.359	0.333	0.353
He-H_2	B_{23}^{00}	1.203[b]	1.171[b]	1.163
	B_{45}^{00}	1.254[b]	1.183[b]	1.093

[a]W. Kolos and L. Wolniewicz, J. Chem. Phys. **46**, 1426 (1967); G. Karl, J. D. Poll, and L. Wolniewicz, Canad. J. Phys. **53**, 1781 (1975); J. D. Poll and L. Wolniewicz, J. Chem. Phys. **68**, 3053 (1978).

[b]Obtained by fitting the long-range part of the calculated dipole moment function.

even the highly regarded, semiempirical potential of Gordon and Shafer.[19]

For the calculations of the CIRTA spectra, it is convenient to separate angular and distance dependences of the dipole moment function by an expansion in terms of spherical harmonics,[5,20,21]

$$\mu_M(\mathbf{r},\mathbf{R})=\frac{4\pi}{\sqrt{3}}\sum_{L,\lambda}A_{\lambda L}(r,R)\times\sum_m Y_\lambda^m(\hat{\mathbf{r}})Y_L^{M-m}(\hat{\mathbf{R}})C(\lambda L\,1;m,M-m). \tag{1}$$

The $C(\ldots;\ldots)$ are Clebsch-Gordon coefficients. In this expression, $\mathbf{r}$ is the vibrational separation of H_2, $\mathbf{R}$ connects He with the center of H_2, $\hat{\mathbf{r}}$ and $\hat{\mathbf{R}}$ are the corresponding unit vectors, and r and R denote the norms of the vectors. We note that for molecules with inversion symmetry the expansion parameter λ must be even. In order to relate the expansion coefficients $A_{\lambda L}$ to the dipole moments calculated in a body-fixed frame, we choose $\hat{\mathbf{R}}$ to be parallel to the z axis. This leads to $M=m$,

$$Y_L^{M-m}=\left[\frac{2L+1}{4\pi}\right]^{1/2},$$

and

$$\mu_M(\mathbf{r},\mathbf{R})=\left[\frac{4\pi(2L+1)}{3}\right]^{1/2}\times\sum_{L,\lambda}A_{\lambda L}(r,R)Y_\lambda^M(\hat{\mathbf{r}})C(\lambda L\,1;M,0)\,. \tag{2}$$

With $\mu_z=\mu_0$ and $\mu_x=-\sqrt{2}\,\mathrm{Re}(\mu_1)$, one also gets

$$\mu_z=\sum_\lambda(\sqrt{\lambda+1}A_{\lambda,\lambda+1}-\sqrt{\lambda}A_{\lambda,\lambda-1})P_\lambda^0(\hat{\mathbf{r}}\cdot\hat{\mathbf{R}})\,, \tag{3}$$

$$\mu_x=\sum_\lambda-[\sqrt{\lambda}A_{\lambda,\lambda+1}+\sqrt{\lambda+1}A_{\lambda,\lambda-1}]\times P_\lambda^1(\hat{\mathbf{r}}\cdot\hat{\mathbf{R}})\left[\frac{(\lambda-1)!}{(\lambda+1)!}\right]^{1/2}. \tag{4}$$

At long range, one finds[20]

$$A_{\lambda,\lambda+1}(r,R)=\alpha q_\lambda(r)\sqrt{\lambda+1}R^{-\lambda-2}\,,\quad A_{\lambda,\lambda-1}=0\,. \tag{5}$$

The short-range exchange and distortion contributions fall off exponentially as a function of the separation R, much like exchange repulsion energies.

The required vibrational matrix elements are defined by

$$B_{\lambda L}^{vv'}(R)=\langle v\,|\,A_{\lambda L}(r,R)\,|\,v'\rangle\,. \tag{6}$$

The weak j dependence of the vibrational functions $|v\rangle$ may safely be neglected for our purpose. Assuming linear variation of the $A_{\lambda L}(r,R)$ over the range of vibrational motion, one gets the r-centroid approximation

$$B_{\lambda L}^{vv'}(R)\simeq A_{\lambda L}(\langle v\,|\,r\,|\,v\rangle,R)\,. \tag{7}$$

For rototranslational spectra we have $v=v'=0$. Thus a first set of induced dipole strengths have been calculated for a fixed $r_0=\langle 0\,|\,r\,|\,0\rangle=1.449$ bohrs.[12] The preliminary results reported in Ref. 22 have been based on this set of calculations. As shown earlier,[14] this choice of the bond distance yields vibrationally averaged quadrupole moments and polarizabilities accurate to 1%. However, the exchange terms have a rather strong, nonlinear dependence on the separation r, and it is not clear whether the r-centroid approximation is of sufficient accuracy for these. For that reason, and also for future calculations of the *vibrational* transition moments, we have undertaken further calculations for the the bond distances $r_\pm=r_0\pm\delta$, with $\delta=2[\langle 0\,|\,(r-r_0)^2\,|\,0\rangle]^{1/2}$, that is $r_+=1.787$ and $r_-=1.111$ bohrs. With this set of three points, zero-point vibrational averaging is quite accurate: assuming the power-series expansion $A(r)=\Sigma_n a_n\rho_n$ with $\rho=r-r_0$, one finds for three equally spaced points [$A_0=A(r_0)$, etc.]

$$\langle A\rangle=A_0+\langle\rho\rangle(A_+-A_-)/2\delta+\langle\rho^2\rangle(A_++A_--2A_0)/2\delta^2+a_3(\langle\rho^3\rangle-\langle\rho\rangle\delta^2)+a_4(\langle\rho^4\rangle-\langle\rho^2\rangle\delta^2)\,. \tag{8}$$

With the choice for δ given above, we get

$$\langle 0\,|\,A\,|\,0\rangle=A_0+\tfrac{1}{8}(A_++A_--2A_0)+0.0009a_3+0.0009a_4\,. \tag{9}$$

Thus, the unknown cubic and quartic expansion coefficients enter with very small weight. (Admittedly, we have missed the perfect choice of the points, $r_+=1.755$ and $r_-=1.143$, which would have made these weights exactly equal to zero.)

We have chosen the angles of 0°, 90°, and 45° for the orientations of the H_2 molecule relative to the intermolecular axis $\mathbf{R}$, for a direct comparison with previous work and the computational advantage of such high-symmetry structures. The resulting dipole moments allow the determination of the spherical tensor components A_{01}, A_{23}, A_{21}, and A_{45}, the four leading terms of the expansion (1). We note that the last term A_{45} is smaller than the largest term by almost 2 orders of magnitude; the truncated terms are believed to be negligible and probably buried in the numerical noise of the calculations. For separations R

between 5 and 6 bohrs, where the spectroscopic interactions take place, we have checked that different sets of orientations—e.g., those for two-point and three-point Gauss-Legendre quadrature—do not modify the leading A_{01} and A_{23} components by more than 1%, while A_{45} may vary by up to 20%.

The resulting dipole components, together with their zero-point averages, are given in Table III. The coefficients $B^{00}_{\lambda L}$ obtained from these are given in Table IV and compared in Fig. 1. For large separations R, the vibrational average of the dipole moments is virtually indistinguishable from their value at r_0. However, near the collision diameter, the vibrational averages are greater by about 2%. Consequently, we expect an increase of the CIRTA intensities by 4% over the results reported previously.[9,22]

For the calculation of spectral profiles an analytical form of the expansion coefficients $B_{\lambda L}$ is desirable. The numerical results can be described quite accurately by a function of the form

$$B(R)=\frac{B^{(n)}}{R^n}+B^{(0)}\exp[a(R-R_0)+b(R-R_0)^2]\,, \qquad (10)$$

which is a slight generalization of the form used by van Kranendonk.[23] The parameter R_0 has been chosen to be close to the collision diameter so that $B^{(0)}$ gives the size of the exchange and distortion dipole contribution at the collision diameter. $B^{(n)}$ accounts for the long-range induction or dispersion contributions, with an n value appropriate for the leading term. It should be noted that the parameter $B^{(n)}$ comprises contributions from higher-order terms as effective at the distances from 7 to 10 bohrs, while the damping of the long-range terms, which is rela-

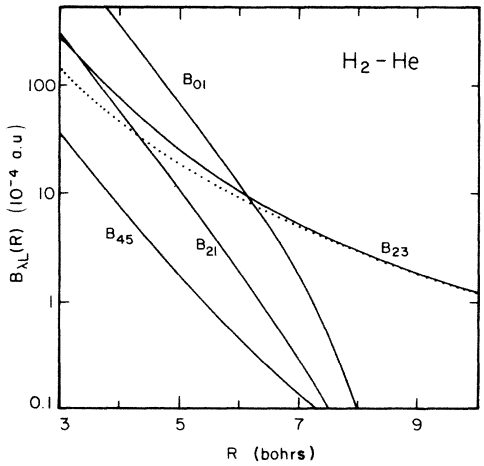

FIG. 1. The four leading dipole components $B^{00}_{\lambda L}(R)=A_{\lambda L}(r_0,R)$ at the fixed bond distance, $r_0=1.449$ bohrs, as function of separation, R. The dotted curve represents the long-range part, Eq. (5), extrapolated to small separations.

TABLE III: Calculated dipole moments[a] in 10^{-6} a.u.

r	R	μ_z at 0°	μ_z at 90°	μ_z at 45°	μ_x at 45°
1.449	3.0	224 785	86 877	146 662	8407
	4.0	55 238	21 511	36 401	−469
	5.0	13 127	3913	8101	−1060
	6.0	3347	201	1674	−694
	7.0	1125	−297	380	−404
	8.0	531	−251	127	−242
	10.0	198	−107	42	−100
1.111	3.0	125 332	59 322	89 386	2369
	4.0	29 764	13 465	21 038	−973
	5.0	6908	2119	4388	−828
	6.0	1812	−4	875	−478
	7.0	659	−222	210	−270
	8.0	333	−169	78	−161
	10.0	131	−69	30	−66
1.787	3.0	366 497	112 415	214 701	17 628
	4.0	92 284	29 816	55 624	667
	5.0	22 376	6009	13 065	−1201
	6.0	5590	525	2815	−920
	7.0	1740	−344	627	−554
	8.0	748	−333	185	−335
	10.0	268	−147	54	−139
$\langle 0\|\mu\|0\rangle$	3.0	229 763	86 576	147 866	8785
	4.0	56 605	21 527	36 843	−393
	5.0	13 486	3947	8247	−1048
	6.0	3430	215	1714	−695
	7.0	1143	−293	389	−405
	8.0	533	−251	128	−243
	10.0	198	−108	42	−100

[a]A positive dipole moment corresponds to a negatively charged H_2 and positively charged He.

TABLE IV. Dipole moment expansion coefficients $B^{00}_{\lambda L}$ (10^{-6} a.u.).

	λL			
R	01	23	21	45
3.0	128 810	27 106	−31 525	4212
4.0	32 034	7871	−6295	909
5.0	6876	2600	−1185	191
6.0	1229	1043	−208	44
7.0	166	512	−39	14
8.0	3	291	−9	5
10.0	−7	116	0	1

tively large only for the weak dispersion term, is absorbed in the second term on Eq. (10). The parameters of the fit are collected in Table V. With these and Eq. (10), the input values from Table IV are reproduced to within 1%, except for the very small values at large separations.

The long-range coefficient $B^{(4)}_{23}$ obtained from this fit is in excellent agreement with the value expected from Eq. (5), with $q_2(r)$ replaced by the vibrational average $\langle 0 \mid q_2 \mid 0 \rangle$ and the well-known properties of the separated systems (Table II). Even the small $B^{(6)}_{45}$ is in fairly close agreement with its proper asymptotic value, Eq. (5). Around the collision diameter the quadrupole-induced B^{00}_{23} term is larger by 20% than the pure long-range expression, Eq. (5). As was stressed by Wormer and van Dijk,[8] these overlap contributions to B_{23} have a much larger effect on the spectral intensities than the short-range term B_{21}, due to interference with the strong long-range induction part. The small values of the parameters b indicate a rather clean exponential behavior. For the main terms B_{01}, B_{23}, and B_{21}, the parameters a are nearly identical which fact supports the intuitive notion that the overlap terms have more or less the same R dependence. The values of a are also in agreement with the empirical ratio $1/aR_0 \simeq 0.105$ obtained by Trafton[2] from a quantum line-shape analysis of the room-temperature data of Kiss *et al.*[24]

$B^{(7)}_{01}$ represents a fit of the isotropic dispersion contributions. Since the damping of the individual dispersion terms D_7/R^7, D_9/R^9, etc. is not known, it is hardly possible to separate these terms from a fit. Moreover, there is no reliable estimate available for the asymptotic value of $B^{(7)}_{01}$ except for the valence-bond result of −62 a.u. obtained by Berns *et al.* for the equilibrium bond length of H_2.[11] Qualitative estimates may be derived from the simple assumption that a dispersion dipole μ corresponds to a shift of the center of the electronic distribution by $\delta = \mu/2e^-$. μ can then be determined from the balance between dispersion energy gain and energy expense for polarization,

$$\nabla_\delta \left[-\sum_n C_{2n} \mid \mathbf{R}+\delta \mid^{-2n} + 2\delta \cdot \vec{\alpha} \cdot \delta \right] = 0 .$$

This yields

$$\mu_1 + \mu_2 \simeq (\vec{\alpha}_1 - \vec{\alpha}_2) \cdot \hat{\mathbf{R}} \sum_n n C_{2n} R^{-2n-1} . \tag{11}$$

With the C_{2n} given by Meyer,[14] one obtains the isotropic $B^{(7)}_{01} = -48.5$, $B^{(9)}_{01} = -900$, and $B^{(11)}_{01} = -10^5$ a.u. This compares reasonably well with the effective $B^{(7)}_{01}$ fitted to −81 a.u. The formula above implies also an anisotropic dispersion contribution in the order of $B^{(7)}_{21} = -8$ a.u. but this value cannot be recovered from a fit because of numerical noise.

The gratifying agreement between the long-range coefficients $B^{00}_{\lambda,\lambda+1}$, Table V, with their exact asymptotic values (Table II) demonstrates that the CI wave function separates correctly for large internuclear distances. As in the case of He-Ar, neither intramolecular nor intermolecular correlation, which may be identified on the basis of the localized HF orbitals, is negligible. From Table VI it can be seen that intramolecular correlation mainly affects B_{23} via the correction of $q_2(H_2)$ and α(He) as discussed above, while the dispersion reduces the isotropic exchange term. At 5 bohrs, where B_{01} is dominant, this reduction amounts to about 15%. A change in sign as predicted by Berns *et al.*[11] for the dispersion contribution is not observed in our calculations.

The dipole data given in Table III allows the calculation of vibrational transition matrix elements $B^{01}_{\lambda L}$ and $B^{02}_{\lambda L}$, which are important for an interpretation of the CIRV bands.[3] This will be taken up in a forthcoming paper.

III. CIRTA SPECTRA: MOMENTS AND LINE SHAPE

Spectral profiles can be computed from the induced dipole components, Tables IV and V, supplemented by a dependable potential model describing the H_2-He interactions. We choose the isotropic part of the *ab initio* surface by Meyer *et al.*[7] This surface was found[16] to reproduce several very accurate measurements as well as, if not better than, other well-known models and must be considered one of the most dependable interaction potentials presently available for the H_2-He system, certainly at the temperatures of interest here (77–300 K).

TABLE V. Fit parameters for $B^{00}_{\lambda L}$, Eq. (7), $R_0 = 5.70$ a.u.

λL	n	$B^{(n)}$	$B^{(0)}$	a	b
01	7	−80.875	0.002 505 1	−1.672	−0.045
23	4	1.173	0.000 233 6	−1.661	−0.066
21	0	0.000	−0.000 359 0	−1.692	−0.011
45	6	1.183	0.000 034 5	−1.819	−0.079

TABLE VI. Correlation effects on B_{01}^{00} and B_{23}^{00} (10^{-5} a.u.).

R (bohr)	5.0		7.0	
λL	01	23	01	23
SCF	809	264	30	53
SCF + intramolecular CI	786	257	30	51
SCF + intramolecular and intermolecular CI	676	255	16	51

The quantum formalism adopted for the line-shape computations is described elsewhere.[5] Within the isotropic potential approximation, it is an exact formalism which has been used extensively for many molecular systems.[22] Since the H_2-He potential[7] does not feature any bound states or narrow scattering resonances, the line shape computation is straightforward.[22] Convergence is obtained by summing over 33 partial waves for the initial state. For every λL value, translational profiles $g_{\lambda L}(\omega,T)$ are obtained from Eq. (22) of Ref. 5 at 15 frequency points, up to frequencies of 1000 cm^{-1}. At negative frequencies, the $g_{\lambda L}$ are obtained without tedious computations from the principle of detailed balance [Eq. (27) of Ref. 5]. The integral over energy is based on 22 energies ranging from $\sim kT/20$ to $\sim 12kT$, where k designates Boltzmann's constant. The CIRTA spectra are then constructed by superimposing the appropriately shifted translational profiles according to Eqs. (21) and (24) of Ref. 5. By variations of the grid widths, etc., the numerical uncertainty of the line-shape computations was estimated not to exceed 1%; for the far wing, at frequency shifts of ~ 1000 cm^{-1}, we estimate a somewhat greater uncertainty of perhaps 2%.

In order to test the results of our line-shape calculations, we have compared the lowest three spectral moments,

$$M_n^{\lambda L}(T)=\int_0^\infty \left[1+(-1)^n \exp\left[\frac{-\hbar\omega}{kT}\right]\right]\omega^n g_{\lambda L}(\omega;T)d\omega\ , \tag{12}$$

(with $n=0,1,2$) of the translational profiles $g_{\lambda L}(\omega;T)$ with their corresponding sum rules.[21] These can be evaluated from potential and dipole moment directly, without computing the spectral profiles. To that end, we use an exact quantum formalism based on radial pair distribution functions which we obtain by numerical integration of the radial Schrödinger equation as described elsewhere.[25] Since these computations are relatively inexpensive, we have attempted to evaluate the sum formulas with an uncertainty not exceeding 0.5%. We note that the integrals over frequency (12) require an estimate of the high-frequency wing which we have obtained by exponential extrapolation of the computed data, $g_{\lambda L}(\omega_i)$, for frequencies $\tilde{\nu} > 1000$ cm^{-1}. This procedure is permissible in all cases quoted in Table VII for the zeroth moment, and for most cases quoted for the first moment. However, with increasing temperature, especially for the broad $\lambda L=01$ and 21 components, the high-frequency corrections of (12) amount to several percent so that the uncertainties arising from this extrapolation begin to determine the overall errors of the values in columns (ii) of Table

TABLE VII. Sum rules. (i) Computed from Eqs. (5) to (7) of Ref. 25. (ii) Spectral integrals, Eq. (12) of this work, using exponential extrapolation at high frequencies.

	M_0 (10^{-62} erg cm^6)		M_1 (10^{-49} erg cm^6/s)		M_2 (10^{-35} erg cm^6/s^2)	
λL	(i)	(ii)	(i)	(ii)	(i)	(ii)
			at $T=77.4$ K			
01	0.514	0.516	1.222	1.235	0.736	(0.758)
21	0.0155	0.0155	0.0380	0.0386	0.0246	(0.0257)
23	0.139	0.139	0.1306	0.1313	0.0586	(0.0595)
45	0.000 46	0.000 43	0.0013	0.0012	0.000 87	(0.000 82)
			at $T=195$ K			
01	1.213	1.217	2.751	2.813	2.421	(2.548)
21	0.0373	0.0375	0.0915	0.0945	0.0856	(0.0918)
23	0.209	0.209	0.231	0.234	0.179	(0.184)
45	0.0010	0.0010	0.0030	0.0031	0.0029	(0.0032)
			at $T=292.4$ K			
01	1.876	1.884	4.149	4.301	4.652	(4.979)
21	0.0590	0.0594	0.1444	0.1519	0.1708	(0.1869)
23	0.2633	0.2622	0.315	0.321	0.327	(0.340)
45	0.0015	0.0015	0.0047	0.0050	0.0058	(0.0065)

VII. This is true to an even greater extent for the second moments, i.e., for all values given in the last column of the table where the high-frequency corrections amount to 20% in the worst case, with errors of similar magnitude. These values are, therefore, put in parentheses for deemphasis of this comparison.

Spectral moments and results of sum formulas are listed in Table VII for comparison. We note an agreement of better than 1%, the uncertainty of the translational profiles $g_{\lambda L}$, under all conditions where the high-frequency extrapolation of the spectral integrals (12) has not introduced errors in excess of $\sim 1\%$. This test is, therefore, a clear indication that the line shape computations are correct as stated.

The computed spectral profiles of the binary CIRTA spectra are shown in Figs. 2–4. The various components labeled $\lambda L = 01$, 21, 23, and 45 are sketched lightly. Their superposition is given by the heavy curve marked "total." We find a most satisfying agreement with Birnbaum's measurements[4] (dots) at all temperatures considered. We note that both theory and measurement are given on an absolute intensity scale; no adjustable parameters have been used for this comparison. The low-frequency part ($\tilde{\nu} \lesssim 300$ cm^{-1}) of the spectra, which is dominated by the isotropic component ($\lambda L = 01$), is for the first time modeled by the fundamental theory with an accuracy of typically better than $\pm 10\%$, our estimate of the uncertainty of the measurement. At the temperatures of 195 and 292 K, the rotational hydrogen lines $S_0(J)$ (with $J = 0, 1, 2$) are also closely modeled by the theory, but with a slightly greater margin ($\sim 15\%$). This may be a reflection of the somewhat lesser precision of the measurement in this frequency band, due to the subtraction of the strong induced $S_0(J)$-line features of H_2-H_2 pairs from the measured absorption of the mixture of hydrogen and helium, which is necessary for the determination of the enhancement spectra of the dissimilar pairs H_2-He. At 77 K, around the $S_0(0)$ and $S_0(1)$ lines, the differences between theory and measurement amount to $\sim 20\%$; the apparent scatter of the data points is not inconsistent with an uncertainty of the low-temperature data of that order. At the higher temperatures, the agreement of theory and measurement is even better. All measurements are reproduced more closely than by the previous calculations based on the SCF induced dipole components; compare with Figs. 1–3 of Ref. 5. The expected improvement due to the new dipole data over the previous SCF work is, therefore, quite evident. Also, a significant improvement relative to our previous data obtained with fixed vibrational separation[9,22] is observed.

The spectral invariants[21,23] obtained from theory are compared in Table VIII with the experimental values. A most satisfactory consistency is observed, well within the

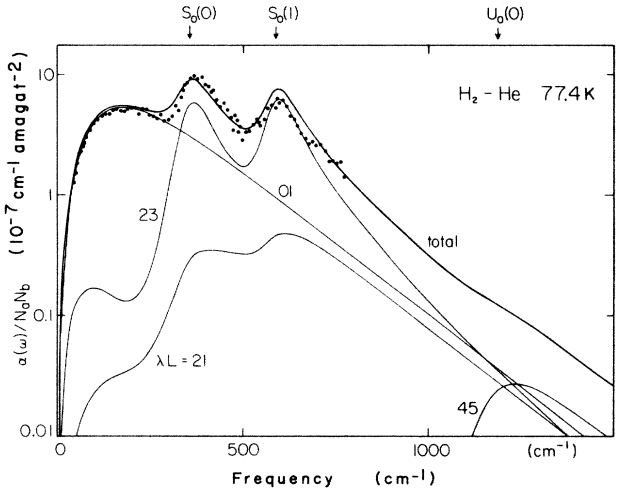

FIG. 2. The absorption coefficient, normalized by the H_2 and He densities, $\alpha(\omega;T)/N_aN_b$, as function of frequency, at 77.4 K. The light curves represent the spectral contributions of each dipole component $B^{00}_{\lambda L}$ which are incoherent with each other. The heavy curve marked total is the sum of these. The dots reproduce the measurement (Ref. 4). The positions of various hydrogen lines $S_0(J), U_0(J)$ which are dipole forbidden in the isolated molecule, are marked in the upper margin.

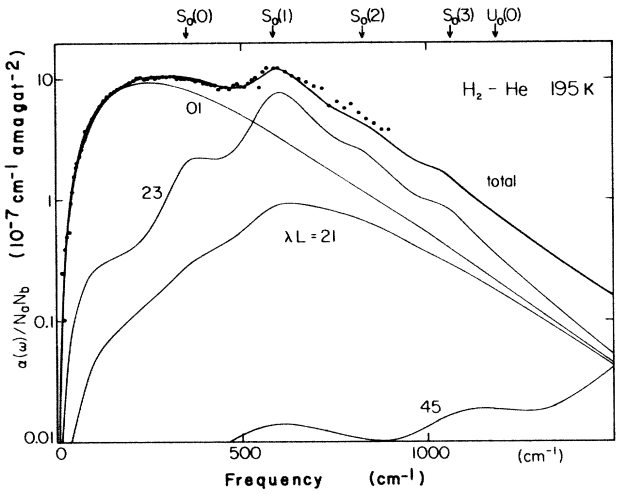

FIG. 3. Same as in Fig. 2, except at the temperature of 195 K.

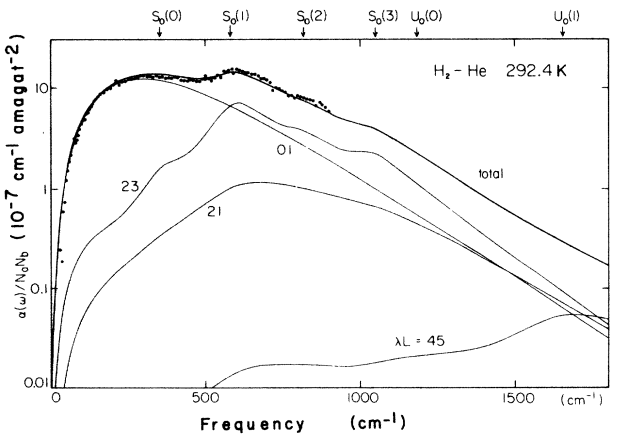

FIG. 4. Same as in Fig. 2, except at the temperature of 292.4 K.

TABLE VIII. Spectral invariants.

T (K)	α_1 (10^{-31} cm^5/s) Expt.[a]	α_1 (10^{-31} cm^5/s) Theory[b]	γ_1 (10^{-58} cm^5 s) Expt.[a]	γ_1 (10^{-58} cm^5 s) Theory[b]
77.4	1.02	1.01	1.29	1.38
195	2.09	1.97	1.18	1.19
292.4	2.86	2.81	1.11	1.19

[a]Based on an analysis (Ref. 28) of Birnbaum's measurement (Ref. 4).
[b]Present work.

estimate of the experimental uncertainties of $\pm 10\%$. For this comparison, we choose the best experimental values obtained in an analysis of Birnbaum's measurement[4] by Cohen *et al.*[26] (labeled "constrained fit" in Ref. 26).

We note that at high frequencies, in the region of the $U_0(J)$ lines of H_2, discernible broad structures are predicted by the theory which arise from the hexadecapole-induced $\lambda L = 45$ component. These features are, however, somewhat uncertain because the $A_{45}(r,R)$ dipole component is by far the weakest one and affected much more than the other components by numerical noise and the truncation of the series, Eq. (2), after four terms. New measurements of the high-frequency wing of these spectra have been obtained recently[27] which are in reasonable agreement ($\sim 20\%$) with the theoretical predictions, for frequencies up to 1700 cm^{-1}.

IV. CONCLUSION

We have computed the dipole moment of the H_2-He molecular system from the fundamental theory with an uncertainty believed to be less than $\pm 2\%$. The CIRTA spectra and spectra moments, which we calculate from these data, and a dependable, isotropic interaction potential, are seen to be in close agreement with Birnbaum's celebrated measurement at 77, 195, and 292 K, well within the uncertainty of the measurement as far as we can determine. The work suggests that reliable predictions of such CIRTA spectra can thus be generated at all temperatures of interest for planetary atmospheres, and over a frequency band which is limited only at the highest frequencies ($\gtrsim 2000$ cm^{-1}) where the less well known $\lambda L = 45$ component, or possibly higher components that are here neglected, dominate the spectra.

In the present work the anisotropy of the interaction potential was neglected. This anisotropy is known to be quite small and may not affect the computed spectra much. Close-coupling calculations which account for the anisotropy in a rather exact way are very expensive but are being undertaken by Meyer and Schäfer.[28] The results indicate a rather minor effect of the anisotropy and seem to largely justify the neglect. Other work[29] based on the distorted-wave approximation is much less rigorous than the close-coupling scheme. It indicates that the effect of the anisotropy affects largely the far wing, but only by a few percent; the spectra shown in Fig. 2 would not discernibly be affected by it. This result also supports the current neglect of the anisotropy.

Previous work[5] based on the SCF dipole moments[8] gave spectral intensities that fall short of the measurements[4] by about 15% when computed with an isotropic, semiempirical potential.[6] When the *ab initio* potential[7] is used instead, a slightly greater discrepancy ($\sim 20\%$) results for the translational spectra ($\omega/2\pi c \lesssim 300$ cm^{-1}), but the rotational spectra are hardly different. We have learned recently that at 77 K, the $\lambda L = 01$ component of Ref. 5 was inadvertantly in error by a few percent[30] so that the discrepancy of the spectra computed with the two potentials[6,7] is in fact somewhat less than Fig. 1 of Ref. 5 suggests. Even with this correction in mind, it is clear that the new dipole data fully account for the defects of the SCF computations and provide a reliable basis for the most accurate computation of such spectra from the fundamental theory.

[1]L. M. Trafton, Astrophys. J. **146**, 558 (1966).
[2]L. M. Trafton, Astrophys. J. **179**, 971 (1973).
[3]H. L. Welsh, *Spectroscopy,* Ser. 1, Vol. 3 of *MTP Int. Rev. Sci., Physical Chemistry,* edited by A. D. Buckingham and D. A. Ramsey (Butterworths, London, 1972).
[4]G. Birnbaum, J. Quant. Spectrosc. Radiat. Transfer **19**, 51 (1978).
[5]G. Birnbaum, S.-I. Chu, A. Dalgarno, L. Frommhold, and E. L. Wright, Phys. Rev. A **29**, 595 (1984).
[6]R. Gengenbach and C. Hahn, Chem. Phys. Lett. **15**, 604 (1972).
[7]W. Meyer, P. C. Hariharan, and W. Kutzelnigg, J. Chem. Phys. **73**, 1880 (1980).
[8]P. E. S. Wormer and G. van Dijk, J. Chem. Phys. **70**, 5695 (1979).
[9]W. Meyer, in *Phenomena Induced by Intermolecular Interactions,* edited by G. Birnbaum (Plenum, New York, 1985).
[10]W. Meyer and L. Frommhold, Phys. Rev. A **33**, 3807 (1986).
[11]R. M. Berns, P. E. S. Wormer, F. Mulder, and A. van der Avoird, J. Chem. Phys. **69**, 2102 (1978).
[12]W. Kolos and L. Wolniewicz, J. Chem. Phys. **41**, 3663 (1964); **43**, 2429 (1965).
[13]G. Karl, J. D. Poll, and L. Wolniewicz, Can. J. Phys. **53**, 1781 (1981).
[14]W. Meyer, Chem. Phys. **17**, 27 (1976).
[15]W. Meyer, R. Ahlrichs, and C. E. Dykstra, in *Advanced Theories and Computational Approaches to the Electronic Structure of Molecules* (Reidl, Dordrecht, 1984).
[16]H. J. Werner and E. A. Reinsch, J. Chem. Phys. **76**, 3144 (1982).
[17]W. Meyer, in *Methods of Electronic Structure Theory,* edited by H. F. Schaefer III, (Plenum, New York, 1978), Vol. IIIa, p. 413.
[18]J. Schäfer and W. E. Koehler, Physica A **129**, 469 (1985), and references therein.
[19]R. Shafer and R. G. Gordon, J. Chem. Phys. **58**, 5422 (1973).
[20]J. D. Poll and J. L. Hunt, Canad. J. Phys. **54**, 461 (1976).
[21]J. D. Poll and J. van Kranendonk, Canad. J. Phys. **39**, 189

(1961).
[22]J. Borysow and L. Frommhold, in *Phenomena Induced by Intermolecular Interactions,* edited by G. Birnbaum (Plenum, New York, 1985).
[23]J. van Kranendonk, Physica **24**, 347 (1958).
[24]Z. J. Kiss, H. P. Gush, and H. L. Welsh, Canad. J. Phys. **37**, 362 (1959).
[25]M. Moraldi, A. Borysow, and L. Frommhold, Chem. Phys. **86**, 339 (1984).
[26]E. R. Cohen, L. Frommhold, and G. Birnbaum, J. Chem. Phys. **77**, 4933 (1982); **78**, 5283 (1983).
[27]G. Birnbaum and H. Bachet (private communication).
[28]J. Schäfer and W. Meyer (unpublished).
[29]M. Moraldi, A. Borysow, J. Borysow, and L. Frommhold, Phys. Rev. A, **34**, 632 (1986).
[30]A. Borysow (private communication).